In Situ Synthesis, Characterization, and Antimicrobial Activity of Silver Nanoparticles Using Water Soluble Polymer

Dipanwita Maity,[1] Mrinal Kanti Bain,[1] Biplab Bhowmick,[1] Joy Sarkar,[2] Saswati Saha,[2] Krishnendu Acharya,[2] Mukut Chakraborty,[3] Dipankar Chattopadhyay[1]

[1]*Department of Polymer Science and Technology, University College of Science and Technology, University of Calcutta, Kolkata-700009, India*
[2]*Department of Botany, Molecular and Applied Mycology and Plant Pathology Laboratory, University of Calcutta, Kolkata-700019, India*
[3]*Department of Chemistry, West Bengal State University, Barasat, Kolkata-700126, India*

Received 28 October 2010; accepted 1 February 2011
DOI 10.1002/app.34266
Published online 15 June 2011 in Wiley Online Library (wileyonlinelibrary.com).

ABSTRACT: A simple and inexpensive, single step synthesis of silver nanoparticles was achieved using poly(methyl vinyl ether-*co*-maleic anhydride) (PVM/MA) both as a reducing and stabilizing agent. The synthetic process was carried out in aqueous solution, making the method versatile and ecofriendly. The synthesized polymer stabilized nanoparticles were stable in water at room temperature without particle aggregation for at least 1 month. The synthesized silver nanoparticles were characterized by UV-visible absorption spectroscopy, X-ray diffraction (XRD), atomic force microscopy (AFM), transmission electron microscopy (TEM), and Fourier transform IR spectroscopy (FTIR). Results showed that Ag-core nanoparticles were coated with PVM/MA shell with thickness of about 5 to 8 nm. The antimicrobial activities of the copolymer (PVM/MA) stabilized silver nanoparticles on various microorganisms were also studied. © 2011 Wiley Periodicals, Inc. J Appl Polym Sci 122: 2189–2196, 2011

Key words: polymer; silver nanoparticles; antibacterial activity; synthesis in green solvents; capping agents

INTRODUCTION

Metal nanoparticles have wide range of applications in various areas of physics, chemistry, material science, and biological science. Intrinsic chemical,[1] optical,[2] electronic,[3] sensing,[4] and catalytic[5] properties of metal nanoparticles largely depend on their shapes and sizes. Recent focus on metallic and semiconductor nanoparticles have been mainly attributed to the so-called quantum size effect[6–9] i.e., their size tunable optical and catalytic properties. Considerable attention was given to the use of metal nanoparticles as building blocks for next generation nano devices.[10] Metal nanoparticles, particularly silver nanoparticles have been the focus of great interest because of their unique optical properties such as their applications to ink-jet printing,[11] electroanalysis of Cytochrome-C,[12] ammonia sensing,[13] herbicide detection,[14] antibacterial performance,[15] and so on.

There are several reported methods for the preparation of silver nanoparticles such as citric acid reduction,[16] electrochemical synthesis,[17] photochemistry,[18] and radiation reduction.[19] But now a days, a molecule which can act both as the reducing and capping agent[20–22] are preferred, since in this case the reaction takes place in one step and there is no need for an external reducing agent. This may enable greater control over the reaction parameters and also condense the number of steps involved in synthesis of the metal nanoparticles. Another focused area of research is accomplishing the nanoparticle formation in the aqueous media.[23] This is important from the environmental point of view with regard to large-scale nanoparticle synthesis. Water based methods offer several advantages over the nonaqueous solvent-based methods such as the ability to solubilize a variety of ions and stabilizer molecules (e.g., surfactants, polymers, and coordinating ligands).[17,24,25]

Chemical resistance and surface modification of these metals nanoparticles with functional polymers i.e., the synthesis of core/shell metal nanoparticles are of significant importance. Core/shell composite nanoparticles are consisted of a core composed of the metal nanoparticle covered by a shell,[26] which may be composed of a variety of material including polymers, inorganic solids, and metals.[27,28] Such materials have been widely used because the

Correspondence to: D. Chattopadhyay (dipanwitamaity@yahoo.co.in).

integrated properties of such materials are better than those of single component counterpart.[29] Ag core nanoparticles have been prepared with the shell of polymer to protect the noble metal silver, which finds extensive use as antibacterial materials, self-depuration materials and activators etc. For example as a promising conductor, silver with large size (~ 100 nm) is widely used as filler to fabricate percolative composite capacitors.[30] The coated polymer shell not only prevents the segregation of silver particles, but also produces excellent compatibility between the filler and the polymer matrix.[30] Encapsulation of silver nanoparticles into poly (methacrylic acid) shell with carboxylate functionality via emulsion polymerization was reported.[31] Furthermore, embedding of metal or inorganic nanoparticles inside the core of conducting polymers such as polypyrrole and polyaniline has become one of the most popular and interesting aspects of nanocomposite synthesis.[32] These materials offer excellent coating suitable materials used in electro catalysis, chemical sensors and microelectronic devices. Silver nanoparticles coated by ultra thin polymers such as polystyrene (Pst) coated silver nanoparticles,[33,34] Ag/C core-shell structured nanoparticles[35] and Ag/PSt core-shell composite nanoparticles[36] have also been reported. However, up to now, there has been no report on the preparation of silver/poly(methyl vinyl ether-*co*-maleic anhydride) core/shell nano particle. The oral toxicity of poly(methyl vinyl ether-*co*-maleic anhydride) (PVM/MA) is quite low (LD50 in guinea pigs is 8–9 g/kg per os from data supplied by ISP Corp.).[37] Poly(methyl vinyl ether-*co*-maleic anhydride) is used as binders for hair sprays. It is widely used in pharmaceutical industries as a thickening and suspending agent, denture adhesive, and adjuvant for transdermal patches.[38] Poly(methyl vinyl ether-*co*-maleic anhydride) can be used for the preparation of particulate dosage forms with bioadhesive or mucoadhesive properties as a biodegradable copolymer.[39] In fact, when polyanhydrides hydrolytically degrade, the product of each cleaved anhydride bond contains two carboxylic acid groups. In accordance with the adsorption theory of adhesion, carboxylic groups would enhance the ability of polymers to form hydrogen bonds with components from the mucosa.[40]

The antimicrobial effects of silver salts have been noticed since antiquity,[41] and silver is currently used to control bacterial growth in a variety of applications, including dental work, catheters and burn wounds.[42,43] Reduction of the particle size of the materials is an efficient and reliable tool for improving their biocompatibility that can be achieved using nanotechnology. The antibacterial property of silver nanoparticles has been studied by a number of microbiologists. Sondi and Salopek-Sondi[44] evaluated the antimicrobial activity of silver nanoparticles against *Escherichia coli.* The results confirmed that the treated *E. coli* cells were damaged, showing pit formation on bacterial cell walls. In another work, Jain and co-workers[45] tested the antibacterial action of silver nanoparticles-coated polyurethane foam and suggested its use as antibacterial water filter. Recently, Hu et al[46] treated cotton fabrics with suspension of silver oxide in chitosan and studied antibacterial actions against *Staphylococcus aureus*.

In this work silver (PVM/MA) core/shell nano particle was synthesized in aqueous medium. The effect of concentration of the precursors, *viz.* the polymer and silver nitrate was studied in detail. The Ag nanoparticles were characterized by UV-Vis spectroscopy, X-ray diffraction (XRD), atomic force microscopy (AFM), and transmission electron microscopy (TEM). The shell was identified using Fourier transform IR (FTIR) spectroscopy and a possible mechanism for the core shell structure is proposed. Our result signifies that Ag nanoparticles synthesized by chemical reduction method, are suitable for formulation of new types of bactericidal materials.

EXPERIMENTAL

Materials and methods

Silver nitrate ($AgNO_3$) and sodium hydroxide (NaOH) were purchased from Merck, India. Poly-(methyl vinyl ether-*co*-maleic anhydride) (PVM/MA) of weight average molecular weight 67,000 was purchased from Aldrich. All the chemicals were used as received without further purification.

Synthesis of silver nanoparticles

The synthesis of colloidal silver nanoparticles involved a simple aqueous phase mixing of $AgNO_3$ to varying concentration of PVM/MA solution and a fixed amount of PVM/MA with varying amount of $AgNO_3$. For the preparation of PVM/MA coated silver nanoarticles (Ag NPs), silver nitrate solutions in mili-Q water ($10^{-2}M$,$10^{-3}M$, and$10^{-4}M$) were slowly added to 1.0 wt % aqueous polymer solution at ambient temperature in glass vessel, the pH value of the solution was adjusted to 8 to 9 by 1(M) NaOH solution in mili-Q water. The glass vessels were wrapped by black paper and kept in dark.

Assay for antimicrobial activity of silver nanoparticles against microorganisms

The silver nanoparticles in water were tested for their antibacterial activity by the agar diffusion method. Six bacterial strains, *Micrococcus luteus* [MTCC 1538], *Bacillus subtilis* [MTCC 736], *Bacillus*

cereus [MTCC 306], *Escherichia coli* [MTCC 68], *Proteus vulgarius* [*MTCC 426]*, and *Pseudomonas aeruginosa* [MTCC 8158] were used for this analysis. These bacteria grown in liquid nutrient agar media (HiMedia Laboratories Pvt. Ltd., Mumbai, India) for 24 h before the experiment were seeded in agar plates by the pour plate technique. Two cups were made using a cork borer (10 mm diameter) at an equal distance and were filled with the silver nanoparticle solution and then incubated at 37°C for 24 h.

Characterization

UV-visible absorption spectroscopy

The nanoparticle formation was monitored by the UV-vis spectra using a UV-vis spectrophotometer system (Agilent 8453 Spectrophotometer). UV-vis study was done using a quartz cell of thickness of 1 cm in the wavelength range (190–1100) nm. The progress of reaction was accompanied by the color change of the reaction mixture within the glass bottle.

X-ray diffraction (XRD)

The sample for X-ray diffraction analysis was prepared by depositing the as prepared sample on a microscopic glass slide and air dried. The diffractogram was then recorded from Seifert XRD 3000P diffractrometer at an accelerating voltage of 35 kV using Cu_α ($\lambda = 1.54$ Å) as X-ray source.

Atomic force microscopy (AFM)

Atomic force microscopic studies of the silver nanoparticle film were performed in a microscope (VEECO, Multimode Nanoscope IIIa) operating in tapping mode (RTESP Tip with resonant frequency 301.78 KHz) to observe the extent of coverage distribution of GNPs in thin film and the morphology and size of the silver nanoparticles.

Transmission electron microscopy (TEM)

The shape, size, and dispersity of the silver nanoparticles were monitored by transmission electron microscopy (HRTEM, model JEM 2010 EM) at an accelerating voltage of 200 kV and fitted with a CCD camera. A specimen for TEM study was made by casting a drop of sample suspension on a carbon coated copper grid and the excess solution were removed by tissue paper and allowed to air dry.

Fourier transform IR (FTIR) spectroscopy

FTIR spectra of samples were recorded by a Shimadzu FTIR-8400S spectrometer. Pellets were prepared by mixing the corresponding dried sample with KBr in a 1 : 100 (wt/wt) ratio.

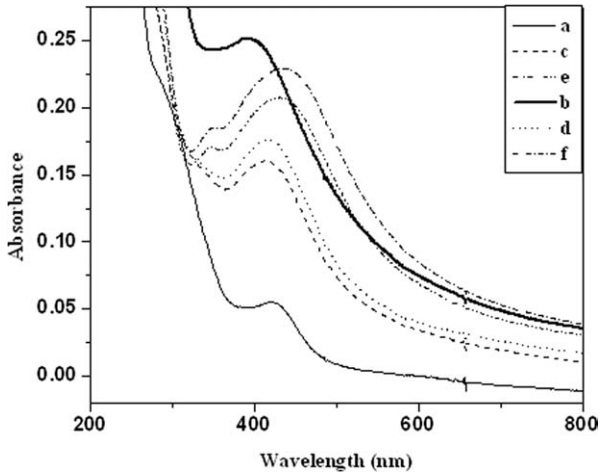

Figure 1 UV-Vis spectra of the colloidal Ag nanoparticles prepared using a fixed concentration of PVM/MA (1.0 wt %) and varying concentration of $AgNO_3$. (a) Initially, using $10^{-2}M$ aqueous solution of $AgNO_3$. (b) After 21 days of aging, using $10^{-2}M$ aqueous solution of $AgNO_3$. (c) Initially, using $10^{-3}M$ aqueous solution of $AgNO_3$. (d) After 21 days of aging, using $10^{-3}M$ aqueous solution of $AgNO_3$. (e) Initially, using $10^{-4}M$ aqueous solution of $AgNO_3$. (f) After 21 days of aging, using $10^{-4}M$ aqueous solution of $AgNO_3$.

RESULTS AND DISCUSSION

UV-visible spectra studies of the as-prepared silver nanoparticles suspensions

The UV-Vis absorption spectra of silver nanoparticle (Ag NPs) solutions at different time interval are depicted in the following figures. In the UV-Vis spectra of the poly(methyl vinyl ether-*co*-maleic anhydride) (PVM/MA) copolymer stabilized silver nanoparticles sample, a peak appears at 424 nm which is analogous to that reported by Lu et al.[47] for the Surface Plasmon Resonance absorption peak of nearly spherical shaped silver nanoparticles which appeared in the vicinity of 425 nm. The appearance of this peak at 424 nm proves that the formed Ag NPs are probably of spherical shapes.

From Figure 1, it is observed that with increasing time at a fixed polymer concentration, the intensity of the peak corresponding to the plasmon resonance absorption of nearly spherical shaped silver nanoparticles increases. This indicates that the number density of the formed Ag NPs increases with time. From Figure 1, also it is seen that using the same polymer concentration with varying $AgNO_3$ concentration, the peak corresponding to the plasmon resonance absorption of the formed Ag nanoparticles almost remain same. So, it can be been concluded that although the formation rate of Ag NPs increases

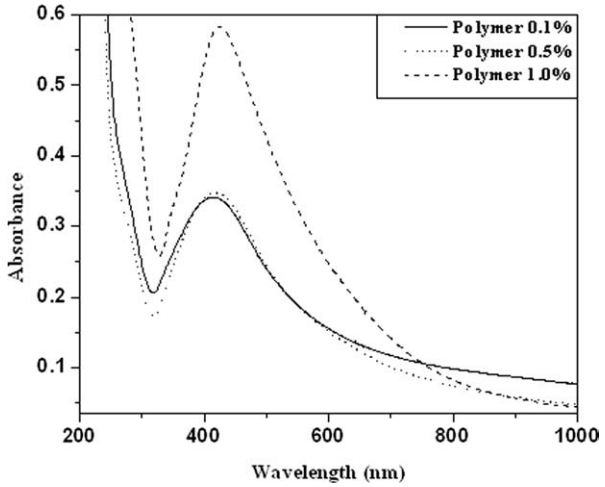

Figure 2 UV-Vis spectra of colloidal Ag nanoparticles at a varying concentration of PVM/MA, keeping the concentration of $AgNO_3$ fixed at $10^{-4}M$.

with time, the shapes and size of the formed nanoparticles remain same.

Figure 2 represents the UV-Vis spectra of Ag NPs prepared using fixed concentration of $AgNO_3$ ($10^{-4}M$) and varying concentration of PVM/MA. From this Figure 2, it can be concluded that with increase in the concentration of polymer, the rate of formation of Ag NPs are faster.

XRD measurements of the as-prepared silver nanoparticles

X-ray diffraction (XRD) analysis was performed to further investigate the crystalline behavior of silver nanoparticles. Representative XRD pattern of the Ag NP are presented in Figure 3 which was nearly identical in all the cases. The peaks observed at $2\theta = 38.45$, 44.45, 64.88, and 77.66° are assigned to (111), (200) (220), and (311) lattice planes of fcc metallic Ag (JCPDF card no. 04-0783) respectively,.[48] In the XRD pattern, the peaks belonging to (200) (220), and (311) lattice planes are quite weak compared with that of (111) plane. The broader weak diffraction peak in small diffraction angle may arise from the amorphous polymer of PVM/MA.

AFM measurements of the as-prepared silver nanoparticles

Figure 4 gives the AFM photographs of silver nanoparticles formed under condition of 1.0 wt % PVM/MA and at an $AgNO_3$ concentration of $10^{-3}M$. The tapping mode AFM image clearly shows the formation of nanoparticle with spherical shape. Owing to agglomeration of particle only approximate sizes are reported. The size of particle is in the range of (40–100) nm.

TEM measurements of the as-prepared silver nanoparticles

The synthesis of the Ag nanoparticles is simply achieved upon ageing the mixture of aqueous $AgNO_3$ and PVM/MA solutions at room temperature. In this ageing process, PVM/MA slowly reduces Ag^+ ions present in the solution to Ag^0 metal. The formation was manifested by a gradual color change of the solution from colorless to yellow. The colloidal suspension was stable for more than a month without any precipitation. The morphology of the AgNPs was observed through transmission electron microscopy (TEM).

Figure 5(a) represents the TEM micrograph of Ag NPs prepared in presence of 0.5 wt % PVM/MA and at an $AgNO_3$ concentration of $10^{-4}M$. It is clear from Figure 5(a) that Ag NPs particles are polydispersed in nature. This suggests that a certain critical concentration of PVM/MA is needed to stabilize the formed Ag NPs in solution. Figure 5(b) represents the TEM micrograph of Ag NPs prepared in presence of 0.5 wt % PVM/MA and with an $AgNO_3$ concentration of $10^{-3}M$. The particles as obtained are larger in size, with respect to those obtained in Figure 5(a). It seems that the larger sized Ag NPs sphere might be formed by the fusion of smaller sized spherical Ag NPs (Ostwald ripening) which is probably why the surface of the larger sized Ag NPs spheres are not smooth and perfectly spherical in shape.

Figure 5(c) represents the TEM micrograph of sample Ag NPs prepared in presence of 1.0 wt % PVM/MA and at an $AgNO_3$ concentration of $10^{-3}M$. As the polymer concentration increases from 0.5 wt % to 1.0 wt % keeping the concentration of $AgNO_3$ fixed at $10^{-3}M$, the formed Ag nanoparticles become much more dispersed i.e., they become much more

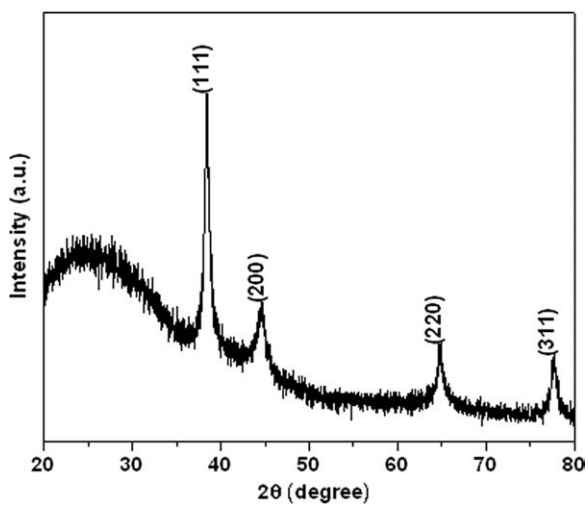

Figure 3 Typical XRD pattern of the core(Ag)/shell(PVM/MA) composite nanoparticles.

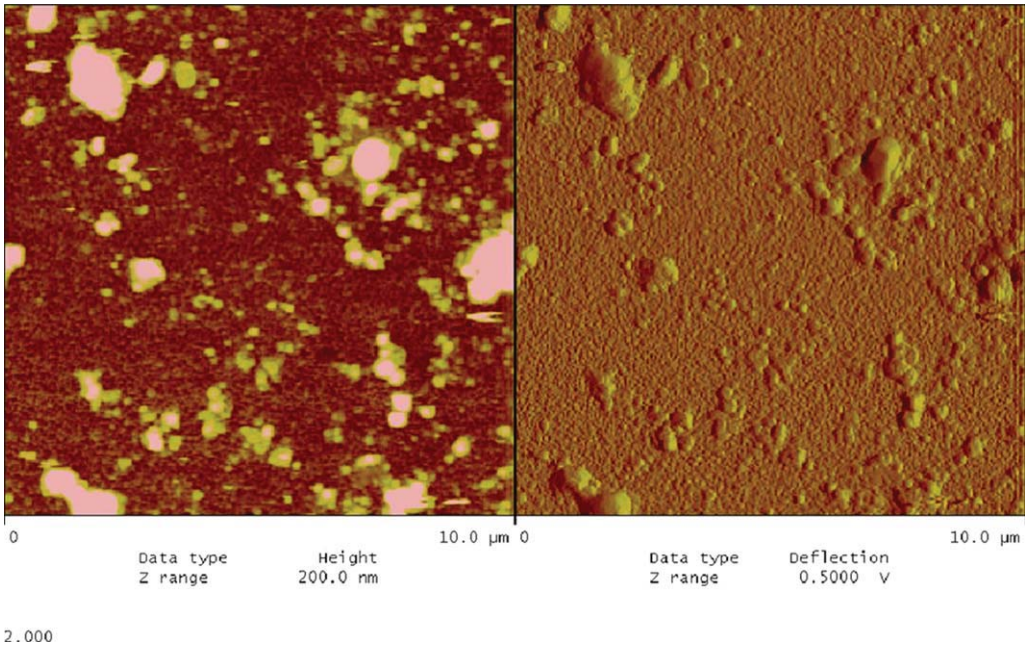

Figure 4 AFM images of Ag nanoparticles produced from reaction mixtures containing (1.0 wt %) PVM/MA + $AgNO_3$ $10^{-3}M$. [Color figure can be viewed in the online issue, which is available at wileyonlinelibrary.com.]

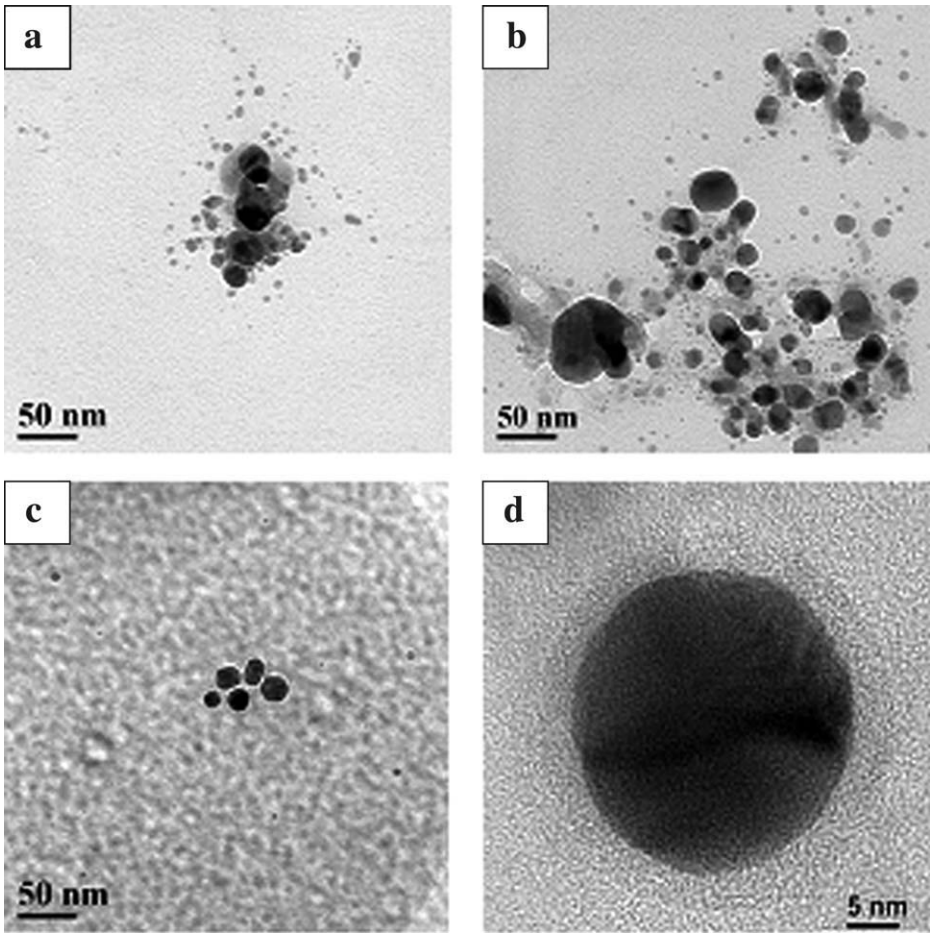

Figure 5 TEM images of Ag nanoparticles produced from reaction mixtures containing (a) (0.5 wt %) PVM/MA + $AgNO_3$ $10^{-4}M$, (b) (0.5 wt %) PVM/MA + $AgNO_3$ $10^{-3}M$, (c) (1.0 wt %) PVM/MA + $AgNO_3$ $10^{-3}M$, (d) blown up image of the section shown in (c).

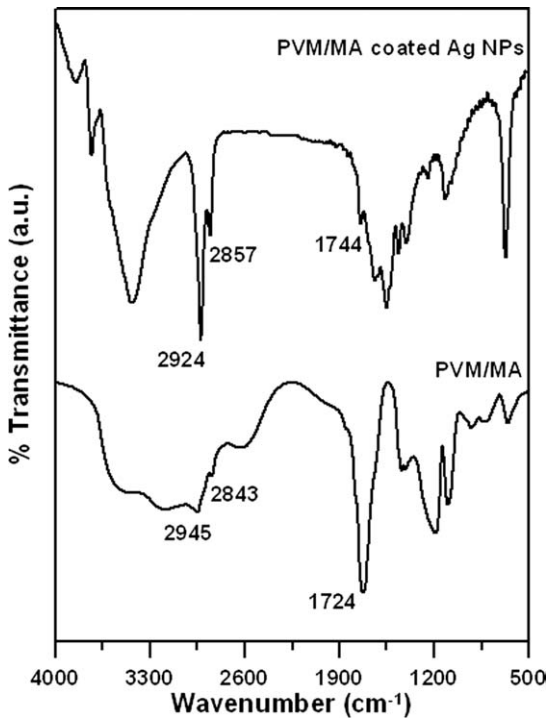

Figure 6 FTIR spectra of PVM/MA and PVM/MA coated Ag nanoparticles.

stable in solution. As expected, with increase in polymer concentration, the shapes of the formed Ag nanoparticles become well defined, *viz.* they become more spherical. The image clearly revealed the formation of spherical shaped Ag NPs of sizes varying from 10 to 40 nm. By close inspection of the TEM images, it can be seen that the formed Ag NPs has a coating of the polymer used on their outer layer. Figure 5(d) is a blown up image of the section shown in Figure 5(c). And obviously enough, with increase in the precursor polymer concentration to 1.0 wt %, the coating of the polymer on the outer wall of the formed Ag NPs become much more prominent, as evidenced by the increase in the shell thickness in TEM. The shell thickness is about 5 to 8 nm. The average diameter of the AgNPs remained almost same with increase in the polymer concentration. TEM images clearly reveal the fact that with increase in precursor $AgNO_3$ concentration from 10^{-4} to $10^{-3}M$, more number of Ag NPs formed in solution i.e., number density of the formed Ag NPs increases.

FTIR spectral analysis of the polymer coated silver nanoparticles

Figure 6 shows the FTIR spectra of the copolymer poly(methyl vinyl ether-*co*-maleic anhydride) and polymer stabilized colloidal Ag nanoparticles. The carbonyl absorption bands of PVM/MA appeared at 1724 cm^{-1}. The peak at 2945 cm^{-1} corresponds to CH_2 asymmetric stretching vibration and the peak at 2843 cm^{-1} corresponds to CH_2 symmetric stretching vibration. In the PVM/MA coated Ag NP sample the peak for carbonyl absorption band appear at 1744 cm^{-1}, whereas the other two peaks appear at 2924 and 2857 cm^{-1}, respectively. Thus IR spectroscopy clearly confirms the presence of PVM/MA on the surface of Ag NPs.

Possible mechanism for the formation of PVM/MA coated silver nanoparticles

The polymer used for the synthesis of Ag NPs (i.e., PVM/MA) has $-OCH_3$ as the pendant group and along with it anhydride group in the backbone of the polymer. So, in this case $-OCH_3$ has a better chance to reduce/stabilize the formation of Ag NPs. This is also supported by the formation of Au NPs by poly(vinyl methyl ether) (PVME),[49] a water soluble polymer similar to poly (methyl vinyl ether-*co*-maleic anhydride) (PVM/MA) used in our case. According to the published literature,[50] the mechanism of Ag NP formation involves the initial reduction of Ag^+ to Ag^0, by the $-OCH_3$ group of PVM/MA. After reducing Ag^+ to Ag^0, the pendant $-OCH_3$ groups of the PVM/MA get converted to a radical cation. This cation accepts an H^+ ion from the solution and forms a protonated species. H-bonding between this protonated species forms the shell structure, as evidenced from the TEM image.

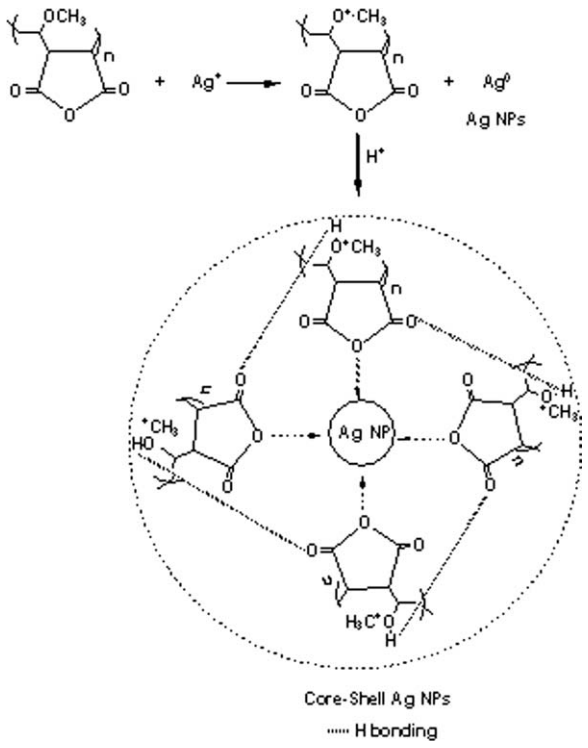

Figure 7 Schematic representation of the formation and stabilization of Ag nanoparticles by PVM/MA.

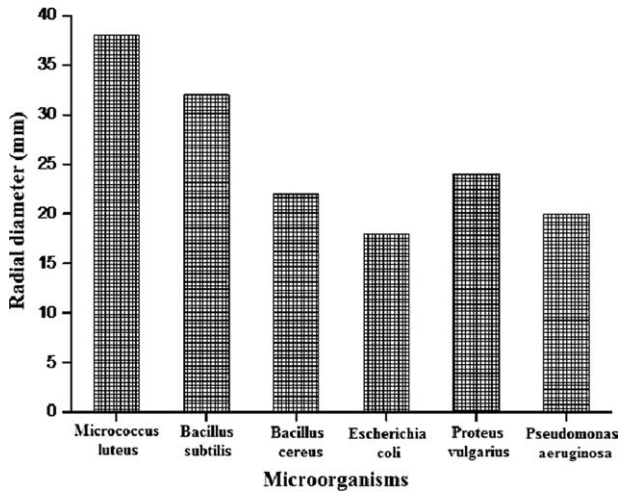

Figure 8 Radial diameter of inhibitory zone by Ag nanoparticles (0.1 mg/mL) against different microorganisms.

Oxygen atom of the anhydride group present in the backbone of the PVM/MA binds to the surface of the as-synthesized Ag NPs and stabilizes it as stable dispersions in aqueous solution. The hydrogen of the protonated -OCH_3 group of PVM/MA and fifth oxygen atom of the anhydride group present in the backbone of the PVM/MA form a self-assemble hydrogen bonded network on surface of the as-synthesized Ag NPs. This is supported by the observation of the shell network in the TEM image. Again, the formation of self-assembled shell network on the outer surface of the as-synthesized Ag NPs is also evidenced from the FT-IR spectroscopy (Fig. 6). The possible pathway for the formation and stabilization of core-shell PVM/MA-Ag nanoparticles is shown in Figure 7.

Antimicrobial activity of the as-prepared silver nanoparticles against microorganisms

The silver nanoparticle solution exhibited excellent antibacterial activity against the bacteria, *M. luteus*, *B. subtilis*, *Bacillus cereus*, *E. coli*, *P. vulgarius*, and *P. aeruginosa* by showing the clearing zones around the cups with bacteria growth on petri plates by cup plate method. Silver nanoparticles at the concentration of 100 μg/mL showed a range of specificity toward its antimicrobial activity (Fig. 8). Results are mean of three separate experiments, each in triplicate. This design of silver nanoparticle synthesis has great potential due to its antibacterial activity.

CONCLUSIONS

In conclusion, spherical shaped Ag nanoparticles have been prepared by wet-chemical reduction of $AgNO_3$ using poly(methyl vinyl ether-*co*-maleic anhydride) (PVM/MA) at room temperature, which is a template-less and seed-less method. The concentration of the polymer used for the reduction has a significant effect on the morphology of the formed Ag NPs. This method can be further extended to prepare other noble metal nanoparticles of various morphologies. Ag nanoparticles prepared by the chemical reduction method described here have great promise as antimicrobial agents. Application of silver nanoparticles based on these findings may lead to valuable discoveries in various fields such as medical devices and antimicrobial agents.

The authors D.M. thank UGC, Government of India for her fellowship, M.K.B. thank for his fellowship under RGNF, UGC scheme, and B.B. thank CRNN, University of Calcutta for his fellowship.

References

1. Jana, N. R.; Gearheart, L.; Obare, S. O.; Murphy, C. J. Langmuir 2002, 18, 922.
2. Xia, Y.; Yang, P.; Sun, Y.; Wu, Y.; Mayers, B.; Gates, B.; Yin, Y.; Kim, F.; Yan, H. Adv Mater 2003, 15, 353.
3. Link, S.; El-Sayed, M. A. J Phys Chem B 1999, 103, 8410.
4. Li, C.-Z.; Male, K. B.; Hrapovic, S.; Luong, J. H. T.; Chem Commun 2005, 3924.
5. Narayanan, R.; El-Sayed, M. A. J Am Chem Soc 2004, 126, 7194.
6. Efros, A. L. L.; Efros, A. L. Sov Phys Semicond 1982, 16, 772.
7. Brus, L. E. J Phys Chem 1986, 90, 2555.
8. Steigerwald, M. L.; Brus, L. E. Acc Chem Res 1990, 23, 183.
9. Wang, Y.; Herron, N. J Phys Chem B 1991, 95, 525.
10. Kamat, P. V. J Phys Chem B 2002, 106, 7729.
11. Shim, I. K.; Lee, Y. I.; Lee, K. J.; Joung, J. Mater Chem Phys 2008, 110, 316.
12. Li, L.; Qiu, P. H.; Cao, X. N.; Jin, L. T. Electrochim Acta 2008, 53, 5368.
13. Dubas, S. T.; Pimpan, V. Talanta 2008, 76, 29.
14. Dubas, S. T.; Pimpan, V. Mater Lett 2008, 62, 2661.
15. Mohan, Y. M.; Lee, K.; Premkumar, T.; Geckeler, K. E. Polymer 2007, 48, 158.
16. Song, W.; Zhang, X.; Yin, H.; Panpan, S. A.; Liu, X. Chin J Chem 2009, 27, 717.
17. Yin, B.; Ma, H.; Wang, S.; Chen, S. J Phys Chem B 2003, 107, 8898.
18. Kutsenko, A. S.; Granchak, V. M. Theor Exp Chem 2009, 45, 313.
19. Henglein, A. Chem Mater, 1998, 10, 444.
20. Si, S.; Mandal, T. K. Chem Eur J 2007, 13, 3160.
21. Si, S.; Bhattacharjee, R. R.; Banerjee, A.; Mandal, T. K. Chem Eur J 2006, 12, 1256.
22. Bhattacharjee, R. R.; Das, A. K.; Halder, D.; Si S.; Banerjee, A.; Mandal, T. K. J Nanosci Nanotechnol 2005, 5, 1141.
23. Dahl, J. A.; Maddux, B. L. S.; Hutchison, J. E. Chem Rev 2007, 107, 2228.
24. Wei, G. T.; Yang, Z. S.; Lee, C. Y.; Yang, H. Y.; Wang, C. R. C. J Am Chem Soc 2004, 126, 5036.
25. Huang, S.; Ma, H.; Zhang, X.; Yong, F.; Feng, X.; Pan, W.; Wang, X.; Wang, Y.; Chen, S. J Phys Chem B 2005, 109 19823.
26. Fleming, M. S.; Mandal, T. K.; Walt, D. R. Chem Mater 2001, 13, 2210.
27. Wang, C. P.; Liu, X. J.; Ohnuma, I.; Kainuma, R.; Ishida, K. Science 2002, 297, 990.
28. Wang, C. P.; Liu, X. J.; Shi, R. P.; Shen, C.; Wang, Y. Z.; Ohnuma, I. Appl Phys Lett 2007, 91, 141904.

29. Hall, S. R.; Davis, S. A.; Mann, S. Langmuir 2000, 16, 1454.
30. Shen, Y.; Lin, Y. H.; Li, M.; Nan, C. W. Adv Mater 2007, 19, 1418.
31. Gangopadhyay, R.; De, A. Chem Mater 2000, 12, 608.
32. Quaroni L.; Chumanov G. J Am Chem Soc 1999, 121, 10642.
33. Zhang, J. H.; Liu, H. Y.; Wang, Z. L.; Ming, N. B.; Mater Lett 2007, 61, 4579.
34. Tian, C. G.; Wang, E. B.; Kang, Z. H.; Mao, B. D.; Zhang, C.; Lan, Y. J Solid State Chem 2006, 179, 3270.
35. Sun, X. M.; Li, Y. D. Langmuir 2005, 21, 6019.
36. Liu, W. J.; Zhang, Z. C.; He, W. D.; Zheng, C.; Ge, X. W.; Li, J. J Solid State Chem 2006, 179, 1253.
37. Cerchiara, T.; Luppi, B.; Chidichinao, G.; Bigucci, F.; Zecchi, V. Eur J Pharm Biopharm 2005, 61, 195.
38. Sharma, N. C.; Galustians, H. J.; Qaquish, J.; Galustians, A.; Rustogi, K. N.; Petrone, M. E.; Chalnis, P.; Garcia, L.; Volpe, A. R.; Proskin, H. M. J Clin Dent 1999, 10, 131.
39. Arbo's, P.; Wirth, M.; Goa, M. A.; Gabor, F.; Irache, J. M. J Controlled Release 2002, 83, 321.
40. Arbo's, P.; Campanero, M. A.; Arangoa, M. A.; Renedo, M. J.; Irache, J. M. J Controlled Release 2003, 89, 19.
41. Silver, S.; Phung, L. T. Annu Rev Microbiol 1996, 50, 753.
42. Catauro, M. J Mater Sci: Mater Med 2004, 15, 831.
43. Crabtree, J. H. Peritoneal Dialysis Int 2003, 23, 368.
44. Sondi, I.; Salopek-Sondi, B. J Colloid Interface Sci 2004, 275, 177.
45. Bosetti, M. Biomaterials 2002, 23, 887.
46. Hu, Z. Mater Res Soc Symp Proc 2006, 920, 0920-S02-03.
47. Hiramatsu, H.; Osterloh, F. E. Chem Mater 2004, 16, 2509.
48. Lu, L.; Kobayashi, A.; Kikkawa, Y.; Tawa, K.; Ozaki, Y. J Phys Chem B 2006, 110, 23234.
49. Bhattacharjee, R. R.; Chakraborty, M.; Mandal, T. K. J Phys Chem B 2006, 110, 6768.
50. Shervani, Z.; Ikushima, Y.; Sato, M.; Kawanami, H.; Hakuta, Y.; Yokoyama, T.; Nagase, T.; Kuneida, H.; Aramaki, K. Colloid Polym Sci 2008, 286, 403.